

PAPER

Fabrication of controlled hierarchical wrinkle structures on polydimethylsiloxane via one-step C_4F_8 plasma treatment

To cite this article: Liming Miao *et al* 2018 *J. Micromech. Microeng.* **28** 015007

View the [article online](#) for updates and enhancements.

Related content

- [Dynamically programmable surface micro-wrinkles on PDMS-SMA composite](#)
Ping-Liang Ko, Fu-Long Chang, Chih-Hung Li *et al.*
- [A facile method for fabrication of responsive micropatterned surfaces](#)
Rdvan Demiryürek, Mariamu Kassim Ali and Gozde Ozaydin Ince
- [Nanotexturing of poly\(dimethylsiloxane\) in plasmas for creating robust super-hydrophobic surfaces](#)
A D Tserepi, M-E Vlachopoulou and E Gogolides

Fabrication of controlled hierarchical wrinkle structures on polydimethylsiloxane via one-step C₄F₈ plasma treatment

Liming Miao¹ , Xiaoliang Cheng¹, Haotian Chen², Yu Song¹, Hang Guo², Jinxin Zhang¹, Xuexian Chen² and Haixia Zhang^{1,2}

¹ National Key Laboratory of Science and Technology on Micro/Nano Fabrication, Institute of Microelectronics, Peking University, Beijing 100871, People's Republic of China

² Academy for Advanced Interdisciplinary Studies, Peking University, Beijing 100871, People's Republic of China

E-mail: zhang-alice@pku.edu.cn

Received 2 August 2017, revised 14 November 2017

Accepted for publication 16 November 2017

Published 12 December 2017



CrossMark

Abstract

We report a simple method for fabricating two-dimensional and nested hierarchical wrinkle structures on polydimethylsiloxane surfaces via one-step C₄F₈ plasma treatment that innovatively combines two approaches to monolayer wrinkle structure fabrication. The wavelengths of the two dimensions of the wrinkle structures can be controlled by plasma treatment (radio frequency (RF) power and plasma treatment time) and stretching (stretching strain and axial stretching), respectively. We also analyze the different interactions between the two dimensions of wrinkle structures with different wavelengths and explain the phenomenon using Fourier waveform superposition. The character of the two dimensions and hierarchy is obvious when the wavelengths of the two wrinkles are different. In surface wetting tests, the hierarchical wrinkle shows great hydrophobicity and keeps the stretching property under 25%.

Keywords: plasma treatment, controlled wavelength, wrinkle interactions, stretchable hierarchical wrinkle on PDMS

 Supplementary material for this article is available [online](#)

(Some figures may appear in colour only in the online journal)

1. Introduction

The micro-textured surfaces of polymers have attracted much attention. This is particularly the case for micro-structures on PDMS, such as controlled wrinkles [1], pyramids [2], micro-pillars [3, 4] or nanotubes [5] with a variety of scientific and technological applications, including triboelectric nanogenerators [6–9], capacitor/resistor effect pressure sensors [2, 4, 10, 11], cell engineering [12, 13] and microfluidics [14–16]. Compared with other conventional micro-structures, the wrinkle has unique advantages for fabrication, such as simple and low-cost mass production. Further, the wrinkle has a dynamic and reversible structure that can easily form a composite structure with other micro-structures and enable electronics to become more stretchable.

Due to the advantages mentioned above, the structure of wrinkles has been widely researched and there are many relevant works concerning fabrication, pattern control, formation principles and theory analysis [17–26]. Recent reports have observed wrinkle structures in the film-substrate system (a stiff layer and a soft layer) [27, 28]. The theory of wrinkle formation was explained by Huang [26]. As the applied compression strain reaches a certain point, the mismatch between the two layers can result in various wrinkle patterns. Cheng *et al* fabricated homogeneous and disordered wrinkle structures by implementing C₄F₈ plasma on an uncured polydimethylsiloxane (PDMS) surface and employed the results in the design of high-performance triboelectric nanogenerators [18]. Shu *et al* used ultraviolet and ozone (UVO) treatment on a pre-stretched PDMS to fabricate stripe-like wrinkles

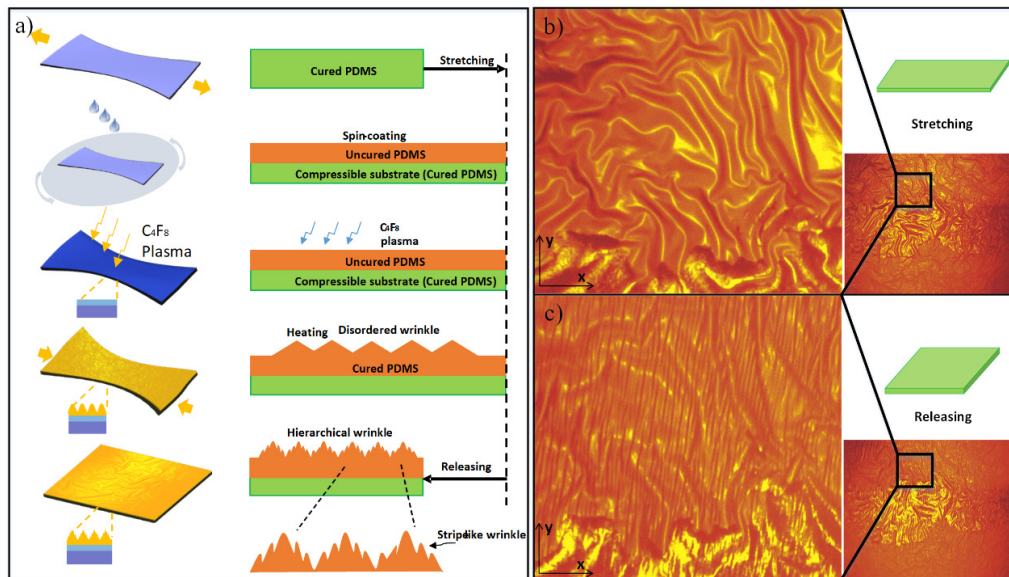


Figure 1. (a) Flowchart and schematic diagram of the fabrication of the hierarchical wrinkle structure via one-step C₄F₈ plasma treatment. (b) Optical photograph the homogeneous and disordered monolayer wrinkle structures (before release). (c) Optical photograph of the hierarchical wrinkle structure (after release).

[22]. By controlling the stretching and releasing axials, heringbone-like and labyrinth-like wrinkle structures can be achieved. Through combining them with existing microstructures on the surface of polymers, Bowden *et al* demonstrated the spontaneous formation of ordered structures in thin films of metals supported on an elastomeric polymer [17]. Using the shape memory effect, Zhao *et al* demonstrated the convenience and flexibility of using shape memory polymers to achieve different wrinkling patterns [26].

The above efforts were focused on monolayer wrinkle structures, but we know that hierarchical wrinkle structures have some features that are better than those of monolayer wrinkle structures and support diverse functions, such as mechanical force sensing, superior hydrophobicity performance [29] and cell stimulation [13]. Moreover, hierarchical wrinkle structures show greater robustness in some stretchable materials, which can then avoid functional failure under continuous stretching.

A composite structure brings various benefits to the hierarchical wrinkle structure, although this has a fabrication cost. The stiff layer in the wrinkle system can be fabricated by using plasma-like UVO or C₄F₈ on the substrate, which is a crucial step to form a mismatch-strain system. Moon *et al* used two UVO plasma steps and two releasing steps to fabricate hierarchical wrinkles [30]. By repeating the ‘stretch–UVO–release’ process twice in two perpendicular directions, Shao *et al* also obtained curvature-induced hierarchical wrinkle structures in soft bilayers [29]. The multi-step plasma treatment makes fabrication a time-costly process in Moon’s work, where it takes about 28 min (2 min for the first plasma treatment and 26 min for the second) to form two-dimensional (2D) and nested hierarchical wrinkle structures.

To obtain high-quality hierarchical wrinkle structures with high efficiency, in this paper we combine two reported wrinkle fabrication methods [1, 18] and create a new method

to form 2D hierarchical wrinkle structures using a single-step C₄F₈ plasma treatment. Figure S1 in the supplementary material (stacks.iop.org/JMM/28/015007/mmedia) shows a comparison of three methods of wrinkle fabrication by C₄F₈ plasma, and table S1 in the supplementary material shows the differences between the fabrication processes for stripe-like wrinkles, disordered wrinkles and hierarchical wrinkles in detail. By spin-coating uncured PDMS on a stretchable substrate-like cured PDMS film, a one-step C₄F₈ plasma treatment can form disordered wrinkle structures and nested stripe-like wrinkles structure with an excellent hydrophobicity property, and the process only takes between 50 s and 10 min. Further, we can control the two dimensions of the wrinkle structures to present different patterns using RF power, plasma treatment time and compression strain. In the fabrication process, we find that changing the wavelength of the two dimensions of the wrinkles can influence the interaction of two wrinkles greatly in the hierarchical wrinkle structure formation process and we analyze this phenomenon by using Fourier waveform superposition theory. The fabricated hierarchical wrinkle structures enable superior hydrophobicity performance with PDMS compared to stripe-like wrinkles and disordered wrinkles, improving the contact angle from 95.68° to 128.58° compared to flat PDMS. After 25% stretching, PDMS with hierarchical wrinkles can still maintain a large contact angle of 126.23°.

2. Fabrication process

A flowchart and schematic diagram of the one-step C₄F₈ plasma fabrication process for hierarchical wrinkle structures is shown in figure 1(a). Firstly, a piece of cured PDMS film of about 2 cm × 4 cm × 1 mm was prepared by heating a mixture of the base solution and curing agent of commercial PDMS (Sylgard 184, Dow Corning Corporation) with a quantity ratio

of 20:1, which makes the PDMS film softer and more stretchable. Secondly, the PDMS film was stretched by 25% and then spin-coated with the uncured PDMS (the quantity ratio of the base solution and curing agent was also 20:1). The thickness of the uncured PDMS was about 10 μm and the thickness of the cured PDMS substrate was 1 mm. Without heating, the cured PDMS covered with uncured PDMS was treated with a C₄F₈ plasma for 150 s and then heated at 80 °C until the uncured PDMS on the surface was cured to form the first kind of disordered and homogenous wrinkle structure. As shown in figure 1(b), with the pre-stretched PDMS released, the second kind of stripe-like wrinkle structure occurred and thus eventually a 2D nested hierarchical wrinkle structure formed. A compressible strain of 25% leads to the compression of the disordered wrinkle in the direction of the stress, while the wrinkle is also to some extent stretched in the direction parallel to the small stripe-like wrinkle because of the positive Poisson ratio. At the same time, a small and regular stripe-like wrinkle structure is formed on the surface of the disordered wrinkle, resulting in a hierarchical wrinkle structure. The compression strain not only changes the original patterns of the disordered wrinkle mechanically, but also adds a new structure on it to form a composite structure that increases the roughness and mechanical sensitivity.

The fluorocarbon plasma treatment was conducted using an inductively coupled plasma (ICP) etcher (Surfacing Technology Systems plc, Multiplex ICP 48443). The gas flow rate and pressure were set at 40 sccm and 3 Pa, respectively. The structure and morphology of the hierarchical wrinkles were characterized using microscopy (Eclipse E200, Nikon Co.) and scanning electron microscopy (SEM, Quanta 600F, FEI Co.). Water contact angle measurements were recorded by a contact angle measurement system (OCA 30, Data Physics Instruments GmbH).

3. Control of hierarchical wrinkle structure

This solitary C₄F₈ plasma treatment step is controllable. Figure S1 in the supplementary material shows the classic model of the wrinkle structure, and we can see that the wrinkle structure can be considered as a sin-like wave pattern with a wavelength and an amplitude. Therefore, to control the surface pattern of the hierarchical wrinkle structure, we need to determine the key process parameters for the wavelength and amplitude. Here, we focus on plasma treatment (RF power and plasma treatment time) and stretching (stretching strain and axial stretching).

3.1. Effect of plasma treatment

The primary role of the RF power is to control the bombarding energy of ions. With increasing RF power, the velocity and density of the particles increase, but the particles become smaller [31–33]. As for the disordered wrinkle, with increasing RF power, more particles bombard the surface of the uncured PDMS, which leads to randomness and fragmentation of the surface and thus the disordered wrinkle grows smaller, as

shown in figure 2. However, from the macroscopic view, the C₄F₈ plasma treatment is also a film deposition process with respect to the chemical reaction between fluorocarbon particles and the uncured PDMS. Due they have the same plasma treatment time (150 s), the thickness of the deposited fluorocarbon layer is approximately the same. Given the wavelength form [22]

$$\lambda = 2\pi h_f \left(\frac{\bar{E}_f}{3E_s} \right)^{\frac{1}{3}} \quad (1)$$

where \bar{E} is the plane strain modulus given by $\bar{E} = \frac{E}{1-\nu^2}$, E is the Young's modulus, ν is the Poisson ratio and h_f represents the stiff film thickness. The subscripts f and s denote the stiff film and the soft substrate, respectively. The same thickness h_f results in the same wavelength of the strip-like wrinkle structure, just as the diagram shows in figure 2(a).

The character of the two dimensions of the wrinkles is also affected by the C₄F₈ plasma treatment time. The disordered wrinkle grows smaller and the wavelength shows a decreasing trend when the C₄F₈ plasma treatment time increases from 50 s to 500 s, as the diagram shows in figure 2(j). In the disordered wrinkle formation process, the deformation caused by the impact of the particles determines the size of the wrinkle. For longer impact times, the deformation will be more fragmented under continuous impact, which is the reason for the phenomenon. While the increasing treatment time leads to a larger thickness of the fluorocarbon layer, which influences the stripe-like wrinkle greatly, and so the wavelength grows larger as the treatment time increases, as the diagram shows in figure 2(j). The optical photographs in figures 2(k)–(n) show that the disordered wrinkles grow smaller as the treatment time increases, while those in figures 2(o)–(r) show that stripe-like wrinkles grow larger as the treatment time increases.

3.2. Effect of stretching

There are important steps—stretching and releasing—that inevitably change the patterns of disordered wrinkle structures. The stretching strain means that the disordered wrinkle structures have to be compressed during release, while the average wavelength in the direction of the x axial shows a decreasing trend. The line of the actual average wavelength of disordered wrinkle structures after release in the direction of the x axial is close to the theoretical line shown in figure 3(a). Further, the optical photographs in figures 3(b)–(e) show the same phenomenon. But, as the classical model calculated, the wavelength of stripe-like wrinkles shows little relationship with the compression strain, as the strain exceeds the critical strain, as demonstrated in figures 3(f)–(i).

The pattern of the hierarchical wrinkle is also dependent on the axial stretching. A disordered wrinkle with a fluorocarbon polymer layer on it rewrinkles into a stripe-on-mountain structure under uniaxial compression. While implementing biaxial stretching at first, a beautiful wrinkle pattern appears that is just like dinosaur skin. The SEM images in figures 3(l)–(q) show the detail of the hierarchical wrinkle structure. The uniaxial compression strain is 25%. In the biaxial compression,

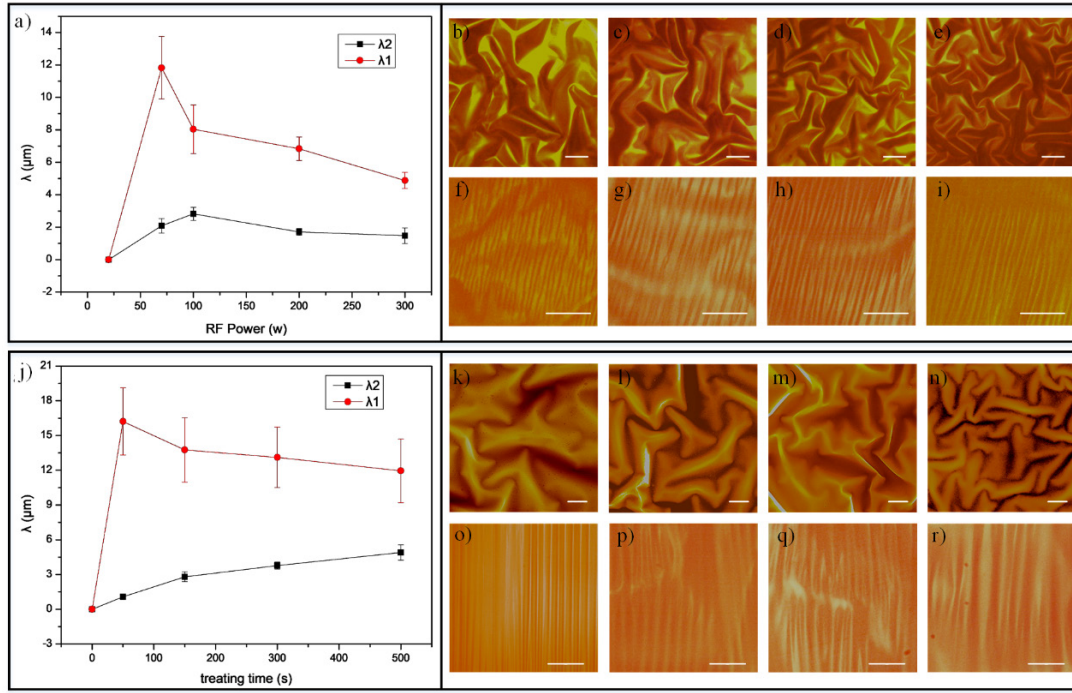


Figure 2. Effect of plasma treatment (RF power (a)–(i) and treatment time (j)–(r)) on two dimensions of wrinkle structures. (a) The wavelength of two dimensions of wrinkle structures as a function of RF power. Labels λ_1 and λ_2 in the diagram represent the average wavelength of the disordered wrinkle structure and the wavelength of the stripe-like wrinkle structure. (b)–(e) Optical photographs of disordered wrinkle structures under increasing RF power (70 W, 100 W, 200 W and 300 W). (f)–(i) Optical photographs of stripe-like wrinkle structures under increasing RF power (70 W, 100 W, 200 W and 300 W). Scale bars, 10 μm . (j) The wavelength of two dimensions of wrinkle structures as a function of C_4F_8 plasma treatment time. Labels λ_1 and λ_2 in the diagram represent the average wavelength of the disordered wrinkle structure and the wavelength of the stripe-like wrinkle structure. (k)–(n) Optical photographs of disordered wrinkle structures under increasing C_4F_8 plasma treatment time (50 s, 150 s, 300 s and 500 s). (o)–(r) Optical photographs of the stripe-like wrinkle structure under increasing C_4F_8 plasma treatment time (50 s, 150 s, 300 s and 500 s). Scale bars, 10 μm .

the strain of both axials (x and y) is 25% and in the releasing process, we first release the strain of the x axial totally and then release the strain of the y axial.

4. Results and discussion

Optical photographs and SEM photographs of the fabricated hierarchical wrinkle structure are shown in figure S3 in the supplementary material. The distribution of the disordered wrinkle is random, while the stripe-like wrinkle is distributed regularly on the parallel direction. The scale of the disordered wrinkle is far larger than that of the stripe-like wrinkle.

4.1. Interaction of two dimensions of the wrinkle

An arbitrary wrinkle pattern can be considered as a superposition of many Fourier components, each of which is designated by a wave number k (or equivalently, wavelength $\lambda = \frac{2\pi}{k}$) [34, 35]. We first consider the disordered and homogeneous wrinkle structure. Assume that the displacement takes the form

$$w(x, y) = W(x, y) \cdot \cos(f(x, y)), \quad (2)$$

through Fourier transformation the displacement takes the form

$$w_D(x, y) = \sum W_{Dk} e^{ik_D r} = \sum W_{Dk} e^{ik_D^x} \cdot e^{ik_D^y}, \quad (3)$$

where the subscript D indicates the disordered wrinkle structure. Since a large number of the particles impact randomly on the surface, the individual particle's influence can be replaced by the average influence of all the particles. That means that the absolute value of the wave number k_D can be replaced by the average absolute value of the wave number $\overline{k_D}$, while the wavelength λ_D of each direction can be replaced by the average wavelength $\overline{\lambda_D}$, and the individual amplitude W_{Dk} can also be replaced by the average amplitude $\overline{W_D}$. The direction of k_D is still different and has random distribution. The hypothesis mentioned above just serves to simplify the model of the disordered wrinkle structure and in fact the fluctuation of the particles' size (like CF_2 or C_3F_6), impulse, carrying charges and effects through scattering cause differences from the assumed model. As for the stripe-like wrinkle structure, the displacement also takes the form

$$w_S(x, y) = W_S e^{ik_S x} \quad (4)$$

and

$$\lambda_S = \frac{2\pi}{k_S}. \quad (5)$$

The subscript S indicates the stripe-like wrinkle structure. The wave form shows no relationship with the direction of the y axial and is a sinusoidal curve in the direction of the x axial. Here, we consider $w_S(x, y)$ to be a Fourier component of the hierarchical wrinkle structure, or, in other words, the

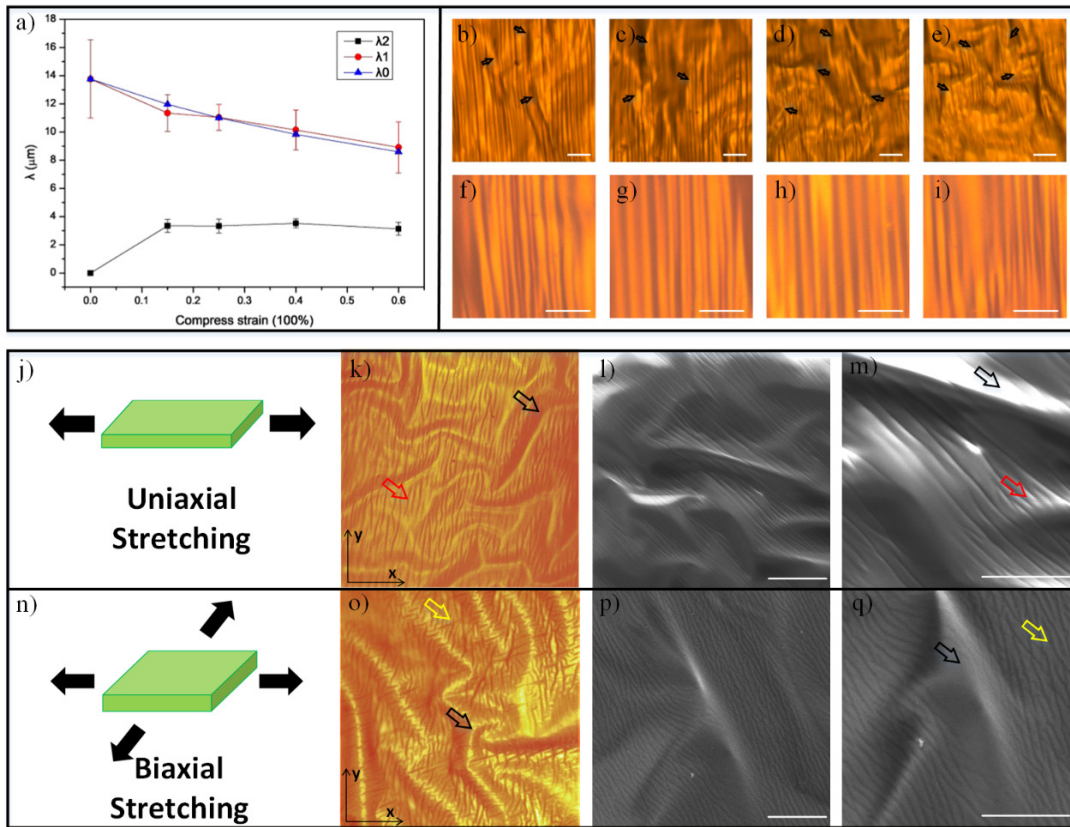


Figure 3. Effect of stretching (stretching strain (a)–(i) and axial stretching (j)–(q)) on two dimensions of wrinkle structures. (a) The wavelength in the direction of the x axial of two dimensions of wrinkle structures as a function of compression strain. Labels λ_0 , λ_1 and λ_2 in the diagram represent the theoretical wavelength of the disordered wrinkle structure, the actual wavelength of the disordered wrinkle structure and the actual wavelength of the stripe-like wrinkle structure. (b)–(e) Optical photographs of the disordered wrinkle structure after releasing under increasing compression strain (15%, 25%, 40% and 60%). The black arrows represent the disordered wrinkle. (f)–(i) Optical photographs of the stripe-like wrinkle structure under increasing compression strain (15%, 25%, 40% and 60%). Scale bars, $10 \mu\text{m}$. (j) and (n) Schematics of two ways of stretching. (k) and (o) Optical photographs of hierarchical wrinkle structure ((k) uniaxial stretching and (o) biaxial stretching). The black arrow represents the disordered wrinkle, while the red and yellow arrows represent the stripe-like wrinkle and the herringbone-like wrinkle, with the same applying below. (l)–(q) SEM images of the hierarchical wrinkle structure ((l) and (m) uniaxial and (p) and (q) biaxial). Scale bars, $10 \mu\text{m}$.

hierarchical wrinkle structure is the result of the wave form superposition of the two kinds of monolayer wrinkle structure. The displacement of the hierarchical wrinkle structure takes the form

$$w_H(x, y) = w_D(x, y) + w_S(x, y) = (\sum W_{Dk} e^{ik_D x} \cdot e^{ik_D y}) + W_S e^{ik_S x}. \quad (6)$$

The subscript H indicates the stripe-like wrinkle structure.

As figure 4 shows, when the wavelength of the stripe-like wrinkle structure λ_S is smaller than the average wavelength of the disordered wrinkle structure $\bar{\lambda}_D$, the superposition of two waveforms results in an obvious 2D hierarchical and nested wrinkle structure, with the disordered wrinkle structure as the base-class wrinkle and the stripe-like wrinkle nesting on it. The component $W_S e^{ik_S x}$ enhances the component with $k_D = k_S$ & $y = 0$ (just in the direction of the x axial) in $\sum W_{Dk} e^{ik_D x} \cdot e^{ik_D y}$. Conversely, when the wavelength of the stripe-like wrinkle structure λ_S is larger than the average wavelength of the disordered wrinkle structure $\bar{\lambda}_D$, the stripe-like wrinkle structure is the base wrinkle and the disordered wrinkle structure is nested on the stripe-like wrinkle. The component $\sum W_{Dk} e^{ik_D x} \cdot e^{ik_D y}$ can be seen as a fluctuation term

added onto the dominant term $W_S e^{ik_S x}$. When the λ_S is close to the $\bar{\lambda}_D$, the hierarchical feature is not obvious. The two dimensions of the wrinkle structures tangle with each other and cause the disordered wrinkle to be as figure 4(d) shows. Due to the influence of the unignored term of $W_S e^{ik_S x}$, the random distribution of the direction of the wave number is untenable. Thus, after wave form superposition, the disordered wrinkle structure is not homogeneous and the stripe-like wrinkle structure becomes morphologically messy instead of showing the regular pattern, because of the disturbance of the disordered wrinkle structure. The schematic in figures 4(a), (c) and (e) shows the two dimensions of the wrinkle structures interacting with each other in different wavelengths.

4.2. Hierarchical wrinkle for surface wetting

In nature, different kinds of micro-structural systems, such as lotus, nepenthes and butterfly wings, show excellent surface wetting properties [36–39]. The composite structure in the hierarchical wrinkle structure also has significant implications for surface-wetting applications. A monolayer wrinkle

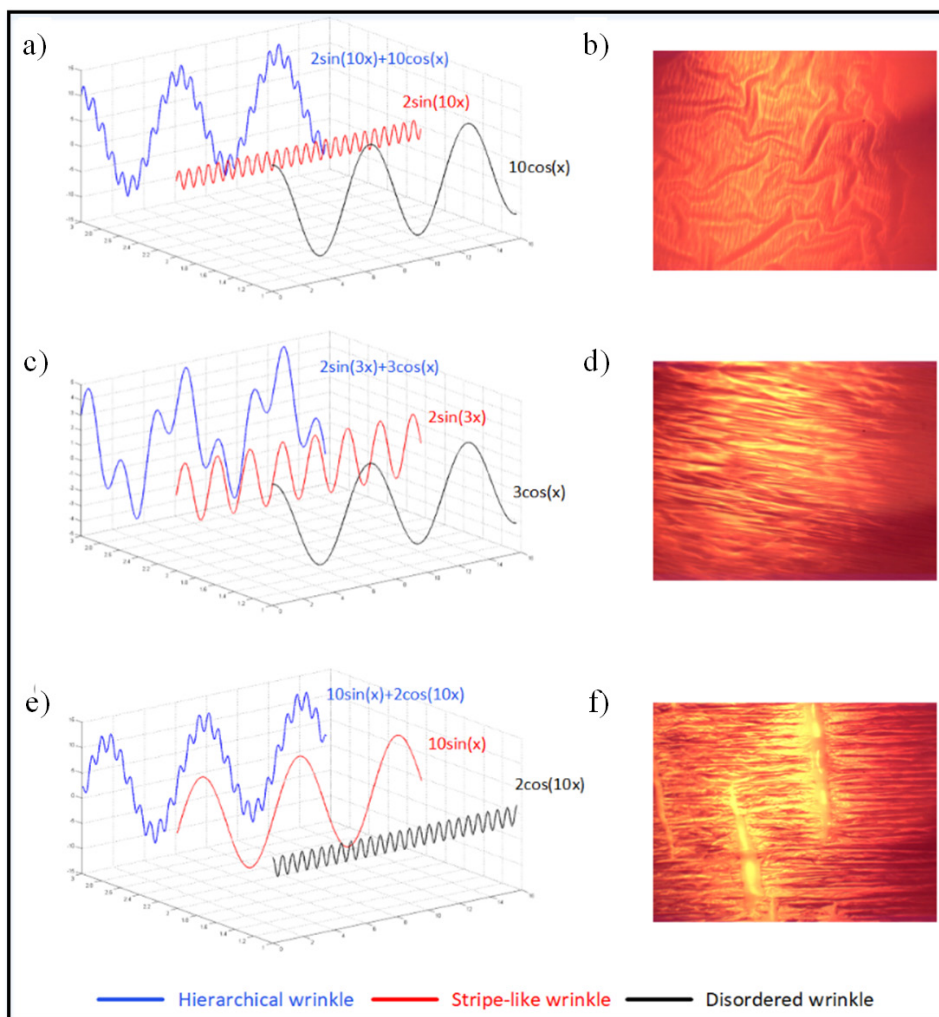


Figure 4. Three states of 2D hierarchical wrinkle structure. (a), (c) and (e) Schematics of simplified waveform superposition to show the interaction between the disordered wrinkle and the stripe-like wrinkle in the formation of the hierarchical wrinkle. (b), (d) and (f) Optical photographs of a hierarchical wrinkle structure fabricated by combining a disordered wrinkle and a stripe-like wrinkle with different wavelengths.

exhibits good hydrophobicity performance, while a hierarchical wrinkle can improve it. Because a stripe-like wrinkle makes the wrinkle pattern the feature of orientation of the water contact angle, we measured the contact angles from two directions: perpendicular and parallel to the stripe-like wrinkle.

Firstly, as figure 5(a) shows, flat PDMS and C4F8 plasma-treated PDMS have contact angles of 95.68 and 108.62°, respectively. As for the monolayer wrinkle, in the direction perpendicular to the stripe-like wrinkle and the disordered wrinkle, the contact angles are 117.53 and 124.52°, respectively. However, the contact angle of PDMS with a hierarchical wrinkle structure can reach about 129.20°, which is greatly improved and better than that of the monolayer wrinkle. After restretching the monolayer wrinkle and hierarchical wrinkle (25% strain), the contact angles of PDMS with stripe-like wrinkle and disordered wrinkles decreases to approximately 108°, which is the exact level of plasma-treated PDMS. By contrast, the hierarchical wrinkle structure still has a contact angle of approximately 126.23°, which demonstrates

the robustness of the hierarchical wrinkle structure in surface wetting applications under stretching. This is because during stretching the monolayer wrinkle (stripe-like wrinkle and disordered wrinkle) become similar to a flat surface, but the hierarchical wrinkle still possesses another disordered wrinkle structure (stripe-like wrinkle), which is crucial for avoiding hydrophobicity function failure.

In the direction parallel to the stripe-like wrinkle, the disordered wrinkle is slightly influenced when stretching, and the water contact angle changes slightly from 123.63° to 121.42°. However, if a liquid is in the crevice, due to the capillary forces the stripe-like wrinkle causes the contact angle to decrease, which also shows its influence on the hierarchical wrinkle structure (the contact angle decreases from 129.20° to 120.77°). When stretching, the water contact angle increases as the stripe-like wrinkle disappears from 120.77° to 125.28°. However, the hierarchical wrinkle structure still shows its excellent hydrophobicity performance when stretching or releasing.

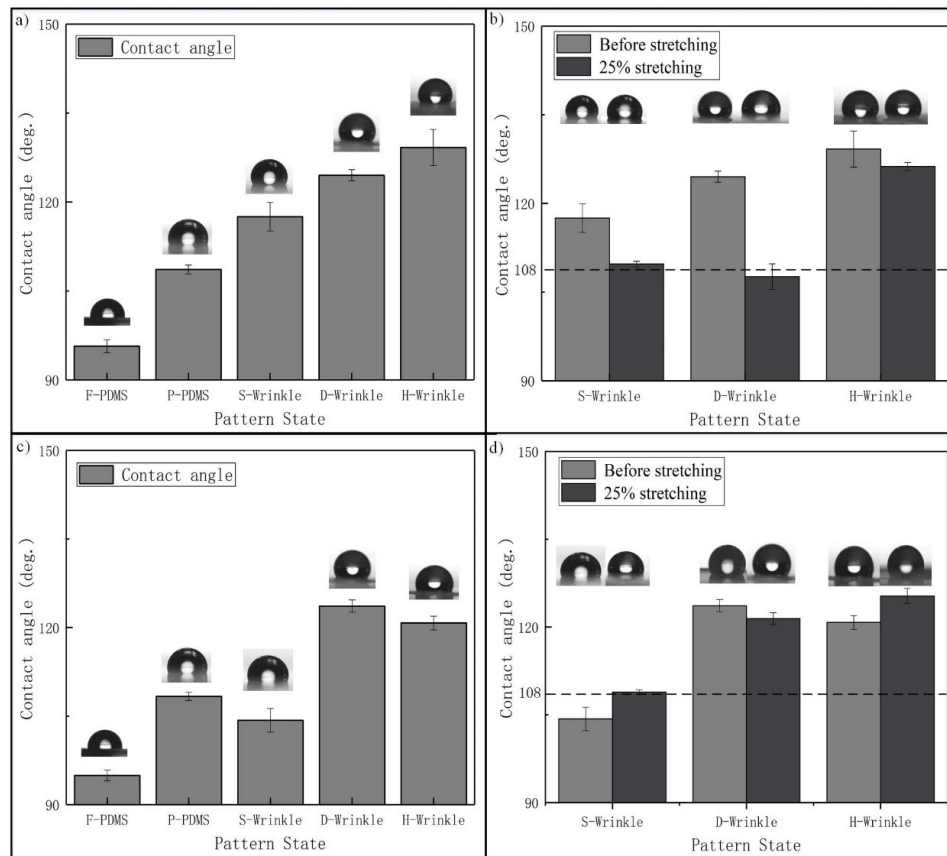


Figure 5. Contact angles of the PDMS surface with different patterns and comparisons among three kinds of wrinkle structure under releasing and 25% stretching. For (a) and (b), the water contact angle is measured perpendicular to the stripe-like wrinkle. For (c) and (d), the water contact angle is measured along the stripe-like wrinkle. (a) For a flat PDMS (F-PDMS) the contact angle is about 95.68° . The plasma-treated PDMS (P-PDMS, without wrinkle structure) has a contact angle of approximately 108.62° . The PDMS with a stripe-like wrinkle (S-wrinkle), a disordered wrinkle (D-wrinkle) and a hierarchical wrinkle (H-wrinkle) shows increasing contact angles of 117.53 , 124.52 and 129.20° , respectively. (b) After restretching (25% strain), the contact angles of the PDMS with a stripe-like wrinkle and a disordered wrinkle obviously decrease to the level of those for the plasma-treated PDMS, with values of 109.73 and 107.62° , respectively. The PDMS with a hierarchical wrinkle still has a contact angle of approximately 126.23° , which demonstrates the robustness of the hierarchical wrinkle structure in surface wetting applications, even under stretching. (c) The contact angles of the flat PDMS, P-PDMS, S-wrinkle, D-wrinkle and H-wrinkle are 94.95 , 108.34 , 104.28 , 123.63 and 120.77° , respectively. (d) After restretching (25% strain), the contact angles of the S-wrinkle, D-wrinkle and H-wrinkle are 108.85 , 121.42 and 125.28° , respectively.

Conclusions

In summary, we have created a new method for fabricating 2D hierarchical and nested wrinkle structures by using a one-step C_4F_8 plasma treatment. Combining the two reported methods for fabricating monolayer wrinkle structures, we have redesigned the manufacturing process and operational procedures by employing key step of spin-coating uncured PDMS on pre-stretched cured PDMS. We compared the differences between the three methods and wrinkle patterns in detail and observed how the disordered wrinkle structure changes into the hierarchical wrinkle structure by looking at the prestretched disordered wrinkle before and after release. The two dimensions of wrinkle structures can be controlled by RF power, C_4F_8 plasma treatment time and compression strain. The wavelength of the disordered wrinkle shows an increasing trend with increasing RF power, while the stripe-like wrinkle scarcely altered. Increasing the C_4F_8 plasma treatment time

results in a decreasing disordered wrinkle wavelength, but the wavelength of the stripe-like wrinkle increases at the same time. By applying increasing compression strain, the wavelength of the disordered wrinkle decreases from $13.76 \mu\text{m}$ to $10.14 \mu\text{m}$, which is similar to the theoretical trend line. Further, we determined the different interactions between two dimensions of wrinkle structures with different wavelengths and analyzed the phenomenon using Fourier wave form superposition theory. When the average wavelength of the disordered wrinkle is dramatically different from the wavelength of the stripe-like wrinkle, the hierarchical wrinkle structure occurs in an obvious way and the hierarchical character is apparent, but when they are close in value, the hierarchical character disappears and the wrinkle structure is more disordered. Finally, the hierarchical wrinkle structure exhibits excellent hydrophobicity and improves the contact angle from 95.68° to 129.20° compared to PDMS with a flat surface. Due to its composite structure, combining two dimensions of wrinkle

structure, the hierarchical wrinkle structure shows excellent robustness in surface-wetting applications and even avoids functional failure under 25% stretching strain.

Acknowledgments

This work was supported in part by the National Key R&D Project from Minister of Science and Technology, China (2016YFA0202701), in part by the National Natural Science Foundation of China (grant nos 61674004, 61176103 and 91323304), in part by the Beijing Science & Technology Project (grant no D151100003315003) and in part by the Beijing Natural Science Foundation of China (grant no 4141002).

ORCID iDs

Liming Miao  <https://orcid.org/0000-0003-2164-5476>

References

- Cheng X, Miao L, Su Z, Chen H, Song Y, Chen X and Zhang H 2017 Controlled fabrication of nanoscale wrinkle structure by fluorocarbon plasma for highly transparent triboelectric nanogenerator *Microsyst. Nanoeng.* **3** 16074
- Zhang J, Shi M, Chen H, Han M, Song Y, Cheng X and Zhang H 2016 Ultra-sensitive transparent and stretchable pressure sensor with single electrode 2016 *IEEE 29th Int. Conf. on Micro Electro Mechanical Systems (MEMS)* pp 173–6
- Lejeune M, Chartier T, Dossou-Yovo C and Noguera R 2009 Ink-jet printing of ceramic micro-pillar arrays *J. Eur. Ceram. Soc.* **29** 905–11
- Tee B C K, Chortos A, Dunn R R, Schwartz G, Eason E and Bao Z 2014 Tunable flexible pressure sensors using microstructured elastomer geometries for intuitive electronics *Adv. Funct. Mater.* **24** 5427–34
- Wang H, Shi M, Zhu K, Su Z, Cheng X, Song Y, Chen X, Liao Z, Zhang M and Zhang H 2016 High performance triboelectric nanogenerators with aligned carbon nanotubes *Nanoscale* **8** 18489–94
- Fan F-R, Lin L, Zhu G, Wu W, Zhang R and Wang Z L 2012 Transparent triboelectric nanogenerators and self-powered pressure sensors based on micropatterned plastic films *Nano Lett.* **12** 3109–14
- Fan F-R, Tian Z-Q and Wang Z L 2012 Flexible triboelectric generator *Nano Energy* **1** 328–34
- Meng B, Cheng X, Zhang X, Han M, Liu W and Zhang H 2014 Single-friction-surface triboelectric generator with human body conduit *Appl. Phys. Lett.* **104** 103904
- Zhang X-S, Han M-D, Wang R-X, Zhu F-Y, Li Z-H, Wang W and Zhang H-X 2013 Frequency-multiplication high-output triboelectric nanogenerator for sustainably powering biomedical microsystems *Nano Lett.* **13** 1168–72
- Schwartz G, Tee B C, Mei J, Appleton A L, Kim D H, Wang H and Bao Z 2013 Flexible polymer transistors with high pressure sensitivity for application in electronic skin and health monitoring *Nat. Commun.* **4** 1859
- Someya T, Sekitani T, Iba S, Kato Y, Kawaguchi H and Sakurai T 2004 A large-area, flexible pressure sensor matrix with organic field-effect transistors for artificial skin applications *Proc. Natl Acad. Sci. USA* **101** 9966–70
- Lam M T, Sim S, Zhu X and Takayama S 2006 The effect of continuous wavy micropatterns on silicone substrates on the alignment of skeletal muscle myoblasts and myotubes *Biomaterials* **27** 4340–7
- Vandeparre H, Gabriele S, Brau F, Gay C, Parker K K and Damman P 2010 Hierarchical wrinkling patterns *Soft Matter* **6** 5751–6
- Gorissen B, Van Hoof C, Reynaerts D and De Volder M 2016 SU8 etch mask for patterning PDMS and its application to flexible fluidic microactuators *Microsyst. Nanoeng.* **2** 16045
- Millet L J, Stewart M E, Sweedler J V, Nuzzo R G and Gillette M U 2007 Microfluidic devices for culturing primary mammalian neurons at low densities *Lab Chip* **7** 987–94
- Yu Y, Ye L, Song Y, Guan Y and Zang J 2017 Wrinkled nitrile rubber films for stretchable and ultra-sensitive respiration sensors *Extreme Mech. Lett.* **11** 128–36
- Bowden N, Brittain S, Evans A G, Hutchinson J W and Whitesides G M 1998 Spontaneous formation of ordered structures in thin films of metals supported on an elastomeric polymer *Nature* **393** 146
- Cheng X, Meng B, Chen X, Han M, Chen H, Su Z, Shi M and Zhang H 2016 Single-step fluorocarbon plasma treatment-induced wrinkle structure for high-performance triboelectric nanogenerator *Small* **12** 229–36
- Hou H, Yin J and Jiang X 2016 Reversible Diels–Alder reaction to control wrinkle patterns: from dynamic chemistry to dynamic patterns *Adv. Mater.* **28** 9126–32
- Khang D-Y, Jiang H, Huang Y and Rogers J A 2006 A stretchable form of single-crystal silicon for high-performance electronics on rubber substrates *Science* **311** 208–12
- Ohzono T, Matsushita S I and Shimomura M 2005 Coupling of wrinkle patterns to microsphere-array lithographic patterns *Soft Matter* **1** 227–30
- Yang S, Khare K and Lin P C 2010 Harnessing surface wrinkle patterns in soft matter *Adv. Funct. Mater.* **20** 2550–64
- Yu S, Sun Y, Ni Y, Zhang X and Zhou H 2016 Controlled formation of surface patterns in metal films deposited on elasticity-gradient PDMS substrates *ACS Appl. Mater. Interfaces* **8** 5706–14
- Huang Z, Hong W and Suo Z 2005 Nonlinear analyses of wrinkles in a film bonded to a compliant substrate *J. Mech. Phys. Solids* **53** 2101–18
- Slesarenko V and Rudykh S 2016 Harnessing viscoelasticity and instabilities for tuning wavy patterns in soft layered composites *Soft Matter* **12** 3677–82
- Zhao Y, Huang W-M and Fu Y-Q 2011 Formation of micro/nano-scale wrinkling patterns atop shape memory polymers *J. Micromech. Microeng.* **21** 067007
- Li Y-N, Kaynia N, Rudykh S and Boyce M C 2013 Wrinkling of interfacial layers in stratified composites *Adv. Eng. Mater.* **15** 921–6
- Lin P-C and Yang S 2007 Spontaneous formation of one-dimensional ripples in transit to highly ordered two-dimensional herringbone structures through sequential and unequal biaxial mechanical stretching *Appl. Phys. Lett.* **90** 241903
- Shao Z-C, Zhao Y, Zhang W, Cao Y and Feng X-Q 2016 Curvature induced hierarchical wrinkling patterns in soft bilayers *Soft Matter* **12** 7977–82
- Moon M-W and Vaziri A 2009 Surface modification of polymers using a multi-step plasma treatment *Scr. Mater.* **60** 44–7
- Kono A and Ohya Y 2000 Photodetachment study of capacitively-coupled RF C4F8 plasma *Japan. J. Appl. Phys.* **39** 1365
- Milella A, Palumbo F, Favia P, Cicala G and d'Agostino R 2004 Continuous and modulated deposition of fluorocarbon films from c-C4F8 plasmas *Plasma Process. Polym.* **1** 164–70

- [33] Suzuki C, Sasaki K and Kadota K 1998 Surface productions of CF and CF₂ radicals in high-density fluorocarbon plasmas *J. Vac. Sci. Technol. A* **16** 2222–6
- [34] Im S H and Huang R 2008 Wrinkle patterns of anisotropic crystal films on viscoelastic substrates *J. Mech. Phys. Solids* **56** 3315–30
- [35] Tanaka T, Sun S-T, Hirokawa Y, Katayama S, Kucera J, Hirose Y and Amiya T 1987 Mechanical instability of gels at the phase transition *Nature* **325** 796–8
- [36] Barthlott W and Neinhuis C 1997 Purity of the sacred lotus, or escape from contamination in biological surfaces *Planta* **202** 1–8
- [37] Bhushan B and Jung Y C 2011 Natural and biomimetic artificial surfaces for superhydrophobicity, self-cleaning, low adhesion, and drag reduction *Prog. Mater. Sci.* **56** 1–108
- [38] Bohn H F and Federle W 2004 Insect aquaplaning: nepenthes pitcher plants capture prey with the peristome, a fully wettable water-lubricated anisotropic surface *Proc. Natl Acad. Sci. USA* **101** 14138–43
- [39] Byun D, Hong J, Ko J H, Lee Y J, Park H C, Byun B-K and Lukes J R 2009 Wetting characteristics of insect wing surfaces *J. Bionic Eng.* **6** 63–70